

Curve Crossing in Collisional Dissociation of Alkali Halide Molecules\*.<sup>†</sup>J. J. EWING,<sup>‡</sup> RICHARD MILSTEIN, AND R. STEPHEN BERRY*Department of Chemistry and the James Franck Institute, The University of Chicago, Chicago, Illinois 60637*

(Received 29 September 1970)

The primary dissociation step for alkali halide diatomics in argon has been studied in order to determine whether collisional dissociation produces ions, atoms, or a mixture of both types of products. The method is based on time-resolved absorption spectroscopy of shock-heated vapors. Results show that the cesium halides, and the rubidium and potassium halides, with the exception of the two iodides, dissociate essentially completely to ions; that the lithium salts and NaI and NaBr dissociate essentially completely to atoms; and that the other alkali halides (KI, RbI, NaCl, and probably NaF) dissociate to mixtures of atoms and ions, at least under some conditions. The branching ratio of atom pairs/ion pairs is interpreted in terms of the effective width of the adiabatic dissociation channel, compared with the spacing of the vibrational levels of the diabatic bound state.

## I. INTRODUCTION

The alkali halide diatomic molecules provide the archetype for the curve-crossing problem.<sup>1</sup> The "ionic" ground states of these molecules are all  ${}^1\Sigma^+$ . The dissociation limit corresponding to the metal ion and the halide ion,  $M^+({}^1S) + X^-({}^1S)$ , differs in energy from that of the atoms  $M^0({}^2S_{1/2}) + X^0({}^2P_{3/2})$  by an amount  $Q$  equal to the difference between the ionization potential I.P. of  $M$  and the electron affinity E.A. of  $X$ ;  $Q = \text{I.P.}(M) - \text{E.A.}(X)$ . Because all ionization potentials of alkali atoms are greater than any electron affinity of a halogen atom,  $Q$  is always positive and the dissociation limit of lowest energy is the atomic limit, for all alkali halides. The combination  ${}^2S_{1/2} + {}^2P_{3/2}$  gives rise to a  ${}^1\Sigma^+$  molecular state, among others. Hence, all alkali halides require at least one crossing, or avoided crossing, of the two  ${}^1\Sigma^+$  potential curves of lowest energy. In the adiabatic or Born-Oppenheimer approximation, the crossing is always avoided according to the noncrossing "theorem," which is essentially a postulate that there are no accidental degeneracies in nature.

The distances  $R_x$  at which the simple Coulomb curve would cross the energy of the separated atoms are shown in Table I for all the alkali halides. For almost all purposes, including our own, these distances can be taken as the crossing distances of the most appropriately defined diabatic curves. It has long been recognized that many of these distances are so great that one cannot expect the atoms  $M$  and  $X$  or ions  $M^+$  and  $X^-$  to interact strongly enough to satisfy the Born-Oppenheimer approximation. It has been suspected for a long time that the electronic wavefunction is unable to switch its character between atomic to ionic, when the nuclei are as far apart as some of the distances in Table I.

Failure of the electronic wavefunction to change adiabatically was involved to explain continuous absorption in the ultraviolet spectrum of the KI molecule, in an energy range where adiabaticity would dictate the existence of discrete spectral bands.<sup>2</sup> Cor-

respondingly, the existence of bands in the absorption spectrum of NaI vapor was rationalized in terms of the validity of the Born-Oppenheimer approximation. In these two cases, the diabatic or adiabatic behavior pertained to the character of the excited electronic state, and depended on assumed assignments of the spectra.

More recently, the curve-crossing behavior of CsBr,<sup>3</sup> of several chlorides,<sup>4</sup> and of CsF<sup>5</sup> were studied by observations of the gaseous molecules, when they were subjected to sudden temperature jumps sufficient to induce dissociation. The chloride work was based on observation of the decay of ultraviolet absorption by the molecules and of visible emission by the neutral alkali atoms. The work on CsBr was based on observations of light absorption by the  $\text{Br}^-$  in its photodetachment continuum and by lines in the principal series of  $\text{Cs}^0$ . The study of CsF used several monitors: infrared bremsstrahlung, absorption by  $\text{F}^-$ , and 4000-Å emission in the process:  $\text{Cs}^+ + e \rightarrow \text{Cs}^0 + h\nu$ . The techniques in the independent CsBr and chloride studies were remarkably similar in other respects: both used incident shock waves in argon to vaporize dilute salt smokes, and then used the reflected shocks to provide the temperature jump leading to dissociation.

The results of the CsBr and CsF work, on one hand, and the chloride work, on the other, were quite different. The inferences based on the chloride work indicated dissociation to atoms at least in the cases of the sodium and potassium salts. The CsBr and CsF studies indicate quite directly that the primary dissociation products of these salts are ions, corresponding to a transient maximum deviation from the population distribution of thermal equilibrium, a completely inverted population, with respect to the two dissociated states in question.

This report describes a systematic study of the primary dissociation process of the alkali halide molecules in argon. We present experimental evidence showing that some alkali halides, such as CsBr, dissociate essentially entirely to ions, that others, such as LiF, dissociate entirely to atoms, and that some, such

TABLE I. Distances  $R_z$ , in au, at which the Coulombic curve of the ionic state,  $M^+X^-$ , crosses the energy of an isolated  $M^0$ ,  $X^0$  atom pair.

	F	Cl	Br	I
Li	14.0	15.3	13.4	11.7
Na	16.1	17.8	15.3	13.1
K	30.6	37.3	27.8	21.3
Rb	37.3	47.7	33.2	24.3
Cs	61.8	97.1	51.3	32.8

as KI, exhibit intermediate behavior, so that both ions and atoms appear in the primary dissociation process. We also show how these observations can be understood theoretically, and how one can predict approximate branching ratios (number of atom pairs/number of ion pairs) for the primary dissociation step. The present work concerns itself for the most part with the primary dissociation process; the later steps are only described in a preliminary way.

## II. EXPERIMENTAL METHODS AND RESULTS

Our method of preparing diatomic alkali halide molecules is based on the use of a shock wave in an argon carrier gas. Most of the details were given in our previous discussion of the dissociation of  $\text{CsBr}^3$ , so we only summarize the description here.

A square tube with inside dimensions of  $3\frac{1}{2}$  in.  $\times$

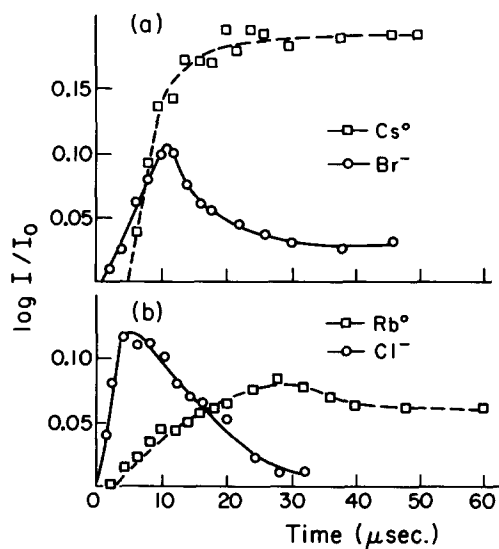


FIG. 1. Time dependence of the concentrations of (a)  $\text{Cs}^\circ$  and  $\text{Br}^-$  in shocked  $\text{CsBr}$  at  $4040^\circ\text{K}$  and 8.5 atm. following the reflected shock; (b)  $\text{Rb}^\circ$  and  $\text{Cl}^-$  from  $\text{RbCl}$ , with final temperature of  $4000^\circ\text{K}$  and 8 atm. These two salts have almost the same crossing distance  $R_z$ , and the two shocks were done to give essentially identical conditions of  $T$  and  $p$ . Both salts dissociate to ions. The differences, which arise both from kinematics and kinetics, have not yet been interpreted.

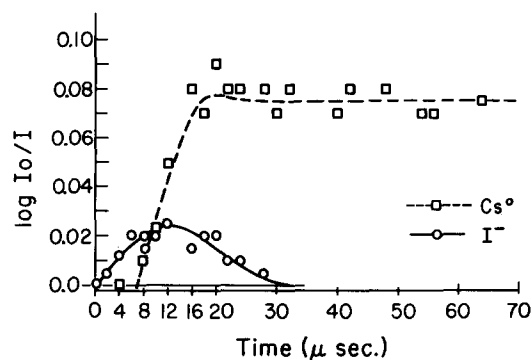


FIG. 2. Time dependence of the concentrations of  $\text{Cs}^\circ$  and  $\text{I}^-$  from  $\text{CsI}$  shocked at  $3000^\circ\text{K}$  and 5.2 atm. Under the conditions of this particular shock, the concentration of  $\text{I}^-$  was too small to give detectable absorption when equilibrium was reached. Nevertheless, the complete primary dissociation to ions is clear.

$3\frac{1}{2}$  in. and length 15 ft is the driven section. A smoke of the salt is prepared in Ar (7–100 torr) by heating salt crystals on a nichrome filament located about 4 in. from the end wall. Convection disperses the smoke through the final 2 ft of the driven section. The concentration of the salt in the incident shock was typically 0.1 mole% of Ar in our experiments.

Mylar or scribed aluminum discs separate the driven section from the driver section. The incident shock, produced by bursting the diaphragm with He or  $\text{H}_2$  at pressures ranging from 75 to 400 psi, heats the gas to a temperature in the range  $1000$ – $2500^\circ\text{K}$  in order to vaporize the salt without dissociating it. These temperatures are high enough to insure that only monomeric molecules are present at equilibrium. Gaseous molecules are observed in the incident shock for at least 15  $\mu\text{sec}$ . This time is long enough to assure that the molecules experience several hundred thousand collisions

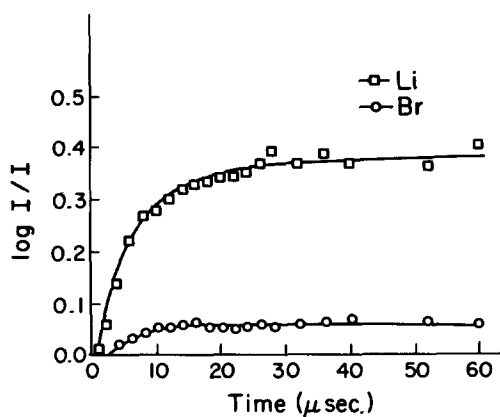


FIG. 3. Time dependence of the concentration of  $\text{Li}^\circ$  and  $\text{Br}^-$  from  $\text{LiBr}$  shocked at  $4850^\circ\text{K}$ . Note that the concentration of  $\text{Li}^\circ$  leads that of  $\text{Br}^-$ , indicating primary dissociation to atoms.

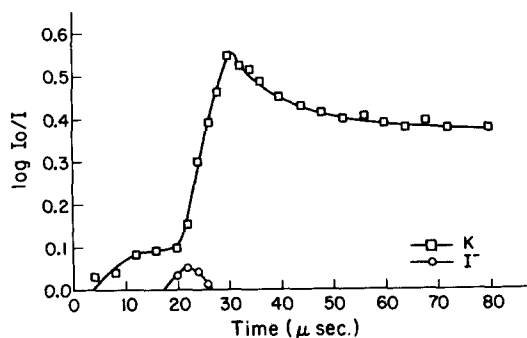


FIG. 4. Time dependence of the concentrations of  $K^0$  and  $I^-$  from KI shocked at  $4800^\circ K$  and 7.1 atm. The  $K^0$  and  $I^-$  are both detectable as soon as the reflected shock reaches the observation point. The concentration of  $I^-$  is too small to give detectable absorption when thermal equilibrium is reached. Note that at time  $t=0$ , the incident shock arrives, and at approximately  $t=18 \mu sec$ , the reflected shock arrives.

and achieve thermal equilibrium. Then the reflected shock returns from the end wall and nearly doubles the temperature. At the new, higher, temperature, a significant fraction (sometimes all) of the molecules are dissociated at equilibrium. It is this sequence of events that we observe.

Our observations have been done primarily by taking time-resolved absorption spectra, monitoring the alkali neutral atoms and the halide ions. Convenient lines of their principal series served for the alkalis, and the photodetachment continua were used for the halides.

In order to measure the Mach number and thus the temperature behind the incident and reflected shocks, pulses from three thermal resistance gauges were ampli-

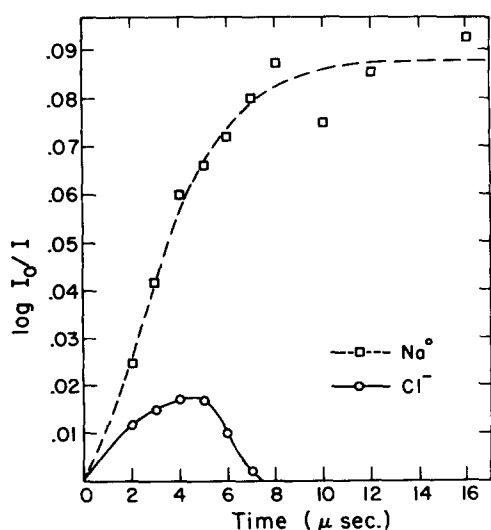


FIG. 5. Time dependence of the concentrations of  $Na^0$  and  $Cl^-$  from NaCl shocked at  $6400^\circ K$  and 1.7 atm. Like Fig. 4, these data imply that NaCl is an intermediate case, at least under the condition of this shock.

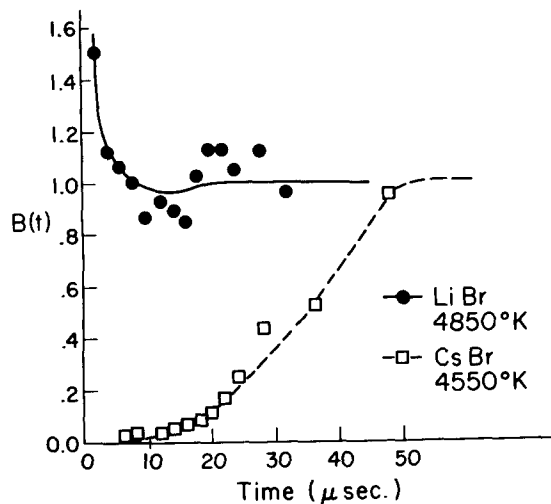


FIG. 6. The observed function  $B(t)$  for case of primary dissociation to ions (CsBr) and a case of primary dissociation to atoms (LiBr).

fied and fed to an oscilloscope. In addition, a delayed pulse ( $\sim 50 \mu sec$ ) from the resistance gauge closest to the end wall, was used to trigger an axially viewed capillary flash lamp. Powered by a  $74\text{-}\mu F$  bank of capacitors charged to  $\sim 6.4 \text{ kV}$ , this flash lamp provided a continuous background for the absorption measurements. Inductors in the transmission line coupling with the capacitors extended the duration of the flash to  $200 \mu sec$ . The intensity of the lamp was essentially constant after the first  $25 \mu sec$ .

The light from the analysis lamp crossed the tube four times or, in some cases, once. The folded light path defined a slab perpendicular to the tube about 1–2 mm thick corresponding to 1–2  $\mu sec$  time resolution. The light entered a rotating drum spectrograph with a slit width of 50–100  $\mu$  and a slit height of 125  $\mu$ . The camera drum, 9 in. in diameter, rotated at 10 000 rpm, corresponding to a film speed of 120  $\mu/\mu sec$ . The time resolution of the apparatus was thus 1–2

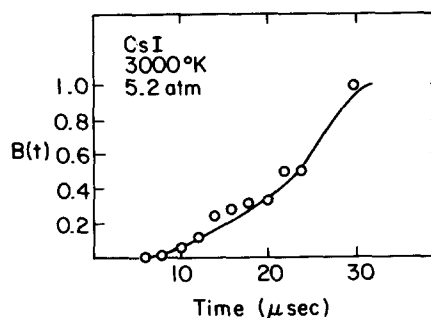


FIG. 7. The function  $B(t)$  for dissociating CsI, an ionic case.

$\mu\text{sec}$ . Spectra were recorded on Kodak 35 mm 103-O film and developed in D-19.

A method of preparing the system similar to ours was used by Hartig, Olschewski, Troe, and Wagner.<sup>4</sup> This group monitored the neutral molecules by following absorption, and alkalis, by following emission as functions of time, with a time resolution of about 15  $\mu\text{sec}$ . We shall return to this point in our concluding remarks.

Results for cesium bromide had previously shown that the appearance of alkali always lagged behind that of halide.<sup>3</sup> Moreover, the halide concentration passed through a true maximum for temperatures of order 3000°K or more. Similar behavior has now been observed for CsF and for CsCl, CsI, RbCl, RbBr, and KBr. Some examples of the time dependence of the concentrations of alkali atoms and halide ions for these salts are shown in Figs. 1-5.

Figures 6-9 show the time dependence of the quantity

$$B(t) = \frac{[M^0(t)]/[M^0]_{\text{equil}}}{[X^-(t)]/[X^-]_{\text{equil}}}, \quad (1)$$

the ratio of the concentrations of  $M^0$  and  $X^-$ , relative to their ratio at equilibrium. The branching ratio for the primary dissociation is the limit of  $B(t)$  as  $t$  approaches zero, the time of passage of the reflected shock. (Strictly, this is true only if no dissociation occurs prior to passage of the reflected shock. In most of our work, this condition was satisfied, but we shall shortly describe experiments in which we observe some dissociation behind the incident shock.) If dissociation occurs entirely to ions,  $B(0) = 0$ ; if dissociation occurs entirely to atoms,  $B(0) \sim \infty$ . Naturally,  $B(t) \rightarrow 1$  as the system approaches equilibrium. Thus  $B(t)$  increases monotonically from 0 to 1 as  $t$  increases from zero, for several alkali halides; for example, see Figs. 6 and 7.

By contrast with the cesium salts, RbCl, RbBr, and KBr, we find that the salts LiBr, LiCl, NaBr, and NaI dissociate to atoms; that is, atomic absorption precedes absorption by negative halide ions for these

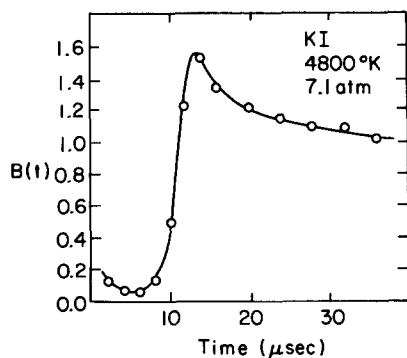


FIG. 8. The function  $B(t)$  for dissociating KI, an intermediate case. The time  $t=0$  corresponds to passage of the reflected shock.

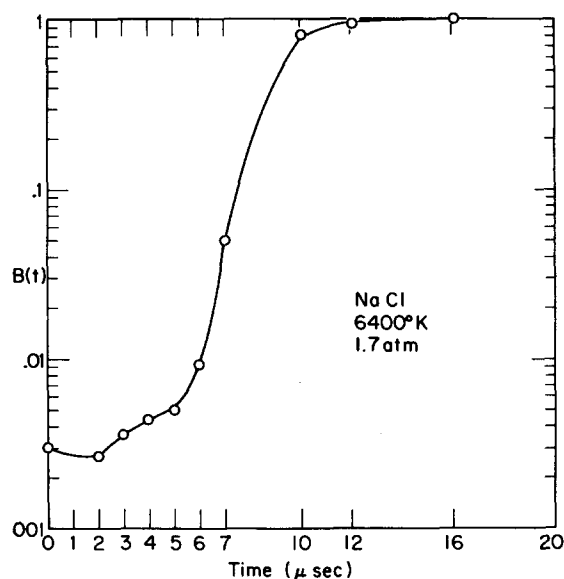


FIG. 9. The function  $B(t)$  for dissociating NaCl, an intermediate case.

salts. Figures 2 and 6 show an example of the time dependence of the concentrations of the alkalis and halides, and of  $B(t)$  in this case. With KBr, neutral K atoms were sometimes detected in the incident shock.

Finally, the salts KI, RbI, and NaCl showed initial dissociation in which both  $M^0$  and  $X^-$  could be detected simultaneously. Under our conditions of concentration and path length the concentration of  $I^-$  and  $Cl^-$  at equilibrium was too small to be detected. In the case of NaCl, only conditions of low pressure (1.7 atm) and high temperature (6400°K) are conducive to producing detectable quantities of  $Cl^-$  in the initial dissociation step. Otherwise NaCl behaves like LiBr, LiCl, NaBr, and NaI and dissociates almost entirely to atoms. Low pressure was necessary in order to slow down the relaxation time for the  $Cl^-$  decay.

As with KBr, these salts showed some dissociation behind the incident shock. Note that in Figs. 1(b), 3, and 4, the concentration of  $M^0$ , as well as that of  $X^-$ , passes through a maximum, indicating that dissociation proceeds faster than ionization. The resulting behavior of  $B(t)$ , as shown in Figs. 6 and 8, is clearly not a monotonic increase or decrease with time. The important point here, however, is that  $B(0)$  appears to have a finite value greater than zero for both these salts.

Thus, in the primary dissociation step, the alkali halides appear to span the full range of behavior, from the extreme of complete dissociation to ions, through intermediate cases with dissociation to atoms and to ions, to the other extreme case of dissociation to atoms only.

We should note here that we have carried out

measurements at several pressure and temperatures for most of the aforementioned salts. The choice of dissociation channel in the primary dissociation step was independent of these variables for the extreme cases. For NaCl, however, this was not the case and we suspect that the value of the branching ratio may be dependent on temperature for the other intermediate cases as well.

### III. INTERPRETATION OF THE BRANCHING RATIO

We now discuss the primary step in the dissociation process, in order to interpret the observed quantity  $B(0)$ , which is a measure of the branching ratio. Strictly, we define the branching ratio  $\beta$  as the ratio of the number of molecules that dissociate into atoms, to the number that dissociate into ions, in the primary dissociation step. We start by computing an effective width,  $E_{AD}$ , of an adiabatic exit channel. This quantity  $E_{AD}$  is the energy bandwidth above the atomic dissociation limit, within which molecules are best described in terms of curves with an avoided crossing, and in which the Born-Oppenheimer approximation is valid. Then we estimate the spacing of the vibrational levels  $E_V$  in the bound (diabatic) Coulomb well, in the energy range of the atomic dissociation limit. Under the conditions of our experiments, vibrational relaxation occurs between two and four orders of magnitude faster than dissociation. This means that dissociation corresponds to a slow peeling off of the sparsely populated high-energy part of a nearly equilibrated vibrational distribution.<sup>6</sup>

Without any detailed assumptions about the density of states in the adiabatic band, we can say that the branching ratio  $\beta$  is given approximately by the ratio of the width of the adiabatic channel  $E_{AD}$  to the spacing of the diabatic vibrational levels in the same region:

$$\beta \cong E_{AD}/E_V. \quad (2)$$

In essence, this says that the vibrationally equilibrated molecules will distribute themselves statistically in the diabatic and adiabatic channels. This relation (2), which can be evaluated theoretically, allows us to assign each of the alkali halides to one of three categories. In the first category,  $\beta \ll 1$ , the adiabatic channel is very narrow compared with the diabatic vibrational level spacing, and the molecules dissociate to ions, skipping over the very narrow adiabatic exit channel. In the second case,  $\beta > 1$ , the adiabatic channel covers many vibrational levels, and the molecules are virtually certain to fall into the adiabatic channel and dissociate to atoms. In the third case,  $\beta \cong 0.1$ , and both the atomic and ionic channels are used in the primary dissociation process. As we shall see, these categories are fairly distinct from each other. Moreover, the theoretical classification corresponds to the behavior as observed in the shock tube experiments.

The theoretical quantity  $\beta$  and the quantity  $B(0)$ ,

based on observed data, are closely related. If there were no free electrons, then the equilibrium constant  $K_1 = [M^0]_{eq}[X^0]_{eq}/[M^+]_{eq}[X^-]_{eq}$  would be equal to  $([M^0]_{eq}/[X^-]_{eq})^2$  and we could set  $\beta^2 = K_1 B^2(0)$ . This approximation is applicable at temperatures less than 3000°K. Whether free electrons are present in significant number during the early stages of dissociation is not known. Preliminary kinetic modeling calculations indicate that it is consistent to assume that electrons are absent in the early stages of dissociation, for about the first 5–10  $\mu$ sec after the passage of the reflected shocks. We therefore assume for purposes of discussion that  $\beta$  is approximately proportional to  $B(0)$ .

This model requires that vibrational relaxation is fast compared to dissociation, and that most collisions do not have sufficient energy to dissociate molecules far down in the potential well. If these requirements are not met, a statistical model must be replaced by a kinetic model which takes into account the specific cross sections for excitation to the various excited energy bands. Such a model is required in *very* high-temperature shocks or in crossed molecular beam experiments where dissociation could be produced by a single collision. Our statistical treatment is expected to be valid for our experiments, where vibrational relaxation requires only 25–500 collisions while the primary dissociation requires tens of thousands of argon-salt collisions.

The quantum mechanical discussion of the diabatic region begins with the arbitrary definition of a transition around  $R_x$ , in which the zero-order, crossing potentials are strongly mixed. The interval in  $R$  space will be given by

$$D = 2 | R_d - R_x |, \quad (3)$$

where we arbitrarily take the internuclear separation  $R_d$  to be the point where the mixing of ionic and atomic zero-order electronic wave functions is  $1/\pi$  times the difference in energy of the zero-order potentials:

$$| H_{ia}(R_d) | = \pi^{-1} | H_{ii}(R_d) - H_{aa}(R_d) |. \quad (4)$$

For the alkali halide potential curves the form of the matrix elements is quite simple:

$$H_{ii}(R_d) = -e^2/R_d, \quad (5a)$$

$$H_{aa}(R_d) = -e^2/R_x, \quad \text{a constant } Q, \quad (5b)$$

$$H_{ia} \cong \text{constant}, \quad (5c)$$

or

$$H_{ia}(R_d) \cong H_{ia}(R_x) R_x/R_d, \quad (5d)$$

where  $e$  is the charge on an electron and  $R_x$  is the crossing distance. Using the relationships [(5a), (5b), and (5d)] and the definition of  $D$  in (3) and (4) we find

$$D = (2\pi/e^2) H_{ia}(R_x) R_x^2. \quad (6)$$

[Assumption (5c) requires that  $D \ll R_x$ ].

We can now define the adiabatic energy band width by using the uncertainty principle in the form of Massey's adiabatic criterion.<sup>7</sup> The adiabatic criterion requires that the time of passage through the crossing region  $D$  be at least as long as the time  $\tau$  determined by the off-diagonal matrix element of the adiabatic (approximate) Hamiltonian  $H_{ia}$ , connecting atomic and ionic states:

$$\tau = \hbar / H_{ia}, \quad (7)$$

if the system is to follow the adiabatic potential curves. If the mean relative velocity of the particles in the region  $D$  is  $v$ , then the adiabatic criterion requires that, for adiabatic behavior,

$$v < v_{\max} = D / \tau \quad (8)$$

or that the kinetic energy of relative motion satisfy

$$\begin{aligned} (\text{KE}) < E_{\text{AD}} &= \mu v_{\max}^2 / 2 \\ &= (\mu / 2) (D^2 H_{ia}^2 / \hbar^2) \\ &= (2\pi^2 / e^4) (H_{ia}^4 R_x^4 / \hbar^2) \mu. \end{aligned} \quad (9)$$

(We let  $\mu$  represent the reduced mass.) Thus, neglecting the difference between the mean relative velocity  $v$  in the region  $D$  and the final relative velocity  $v_f$ , we define the *adiabatic bandwidth*  $E_{\text{AD}}$ , as the width of the energy band within which the motion of the particles follows the adiabatic potential curves. Molecules with final kinetic energy greater than  $E_{\text{AD}}$  cannot dissociate until they reach the higher-energy ionic limit.

One can, incidentally, define an adiabatic channel width from the Landau-Zener expression<sup>8</sup> for the transition probability for diabatic behavior (curve crossing) in a single passage through the transition region:

$$P_{\text{LZ}} = \exp[-2\pi H_{ia}^2 / \hbar v (d/dR) (H_{ii} - H_{aa})]. \quad (10)$$

We define the adiabatic channel width as that final kinetic energy band at the top of which the probability of diabatic behavior reaches  $e^{-1}$ . This definition leads immediately to a value of the velocity  $v_{\max}$  of  $(2\pi/e^2\hbar) H_{ia}^2 R_x^2$  and an energy  $E_{\text{AD}}$  exactly equivalent to Eq. (9).

The calculation of  $E_{\text{AD}}$  and  $\beta$  from theory is clearly acutely sensitive to the calculation of  $H_{ia}$ . Particularly because of the large internuclear distances for which one wants to know  $H_{ia}$ , the accurate evaluation of this matrix element is rather difficult. We have taken adiabatic splittings  $\Delta E^0$  from graphs by Herschbach and Grice<sup>9</sup> to evaluate  $E_{\text{AD}}$  and then to classify the alkali halides. Essentially,  $H_{ia} = \Delta E^0 / 2$ . Herschbach and Grice used three methods to evaluate  $\Delta E^0$  for most of the molecules and two methods for the iodides. The methods are based on wave functions for the metal atoms of Bates and Damgaard.<sup>10</sup> The method giving the largest values of  $\Delta E^0$  makes use of numerical Hartree-Fock functions<sup>11</sup>; a second method, which gives the smallest values, was based on analytic

TABLE II. Energy differences  $\Delta E^0$  between the two lowest  ${}^1\Sigma^+$  states, in the adiabatic approximation, at the distance  $R_x$  at which the two diabatic curves would cross. Values were taken from calculations by Herschbach and Grice (Ref. 9). The three sections of the table A, B, and C, are based on three different methods of computation, as described in the text. Note that  $\Delta E^0 \approx 2H_{ia}$ . Units are  $\text{cm}^{-1}$ : vs means less than  $10^{-2} \text{cm}^{-1}$ .

	F	Cl	Br	I
A.				
Li	280	220	890	2200
Na	110	0.70	3.3	1400
K	0.22	vs	0.20	55
Rb	vs	vs	0.02	1.8
Cs	vs	vs	vs	0.65
B.				
Li	87	76	280	...
Na	26	22	96.0	...
K	0.083	vs	0.087	...
Rb	vs	vs	vs	...
Cs	vs	vs	vs	...
C.				
Li	170	110	460	1500
Na	59	38.0	170	980
K	0.054	vs	0.44	20
Rb	vs	vs	vs	4.5
Cs	vs	vs	vs	0.11

Hartree-Fock functions<sup>12</sup> for all but the iodides, and a third method, giving intermediate values, was based on a new asymptotic expansion. These values of  $\Delta E^0$  are collected in Table II(A.-C.), respectively. From these, we can get some ideas of the range of values that  $E_{\text{AD}}$  can assume. The computed values of  $E_{\text{AD}}$  are given in Table III.

Calculations of the approximate vibrational spacings in the diabatic Coulomb wells are straightforward; the level spacings for a particle in a Coulomb well are

$$E_v = 2\mu\text{Ry} / n^3 m_e,$$

where  $\mu$  is again the reduced mass, Ry is the Rydberg constant,  $m_e$  is the electron mass and  $n$  is the effective principal quantum number at the energy of interest. In our case, we are interested in the energy  $E = -Q$ , the energy of the atomic dissociation limit, so that, neglecting the repulsive part of the potential, we have

$$n = (\mu\text{Ry} / Q m_e)^{1/2}$$

and

$$E_v = 2Q^{3/2} (m_e / \mu\text{Ry})^{1/2}.$$

Vibrational level spacings of the alkali halides, so calculated at the energies  $-Q$ , are given in Table IV.

We now collect our calculations and predict whether dissociation of the salt will be adiabatic, to atoms, or

TABLE III. Adiabatic channel widths,  $E_{AD}$ , based on the values of the corresponding adiabatic splittings  $\Delta E^0$  from Table II. Values are in  $\text{cm}^{-1}$ : "vs" implies  $E_{AD} < 10^{-6} \text{cm}^{-1}$ . The three parts (A-C) are based on the three values of  $\Delta E^0$ , as indicated in the text.

	F	Cl	Br	I
A.				
Li	220	130	23 000	480 000
Na	18	5.8	20 000	360 000
K	vs	vs	$4.1 \times 10^{-5}$	9.5
Rb	vs	vs	vs	0.033
Cs	vs	vs	vs	$3.4 \times 10^{-6}$
B.				
Li				
Li	2.0	1.9	240	...
Na	0.058	0.054	150	...
K	vs	vs	vs	...
Rb	vs	vs	vs	...
Cs	vs	vs	vs	...
C.				
Li	32	9.3	1600	100 000
Na	9.5	0.57	1600	71 000
K	vs	vs	vs	0.39
Rb	vs	vs	vs	$1.3 \times 10^{-4}$
Cs	vs	vs	vs	vs

diabatic, to ions. Note that the results are far more sensitive to  $E_{AD}$  than to  $E_V$ . [In fact, it is clearly preferable to use experimental values of  $B(0)$  to determine  $H_{ia}$  and  $\Delta E^0$ , rather than the reverse.] If the vibrational energy spacing is much much larger than the adiabatic channel width, the chance of a molecule falling into the adiabatic band will be vanishingly small and dissociation should proceed to ions. This condition holds for all Cs salts, KF, KCl, KBr, RbF, RbCl, and RbBr. Possibly RbI should be in this class but classification depends strongly on the choice of wave functions used to calculate adiabatic channel width. On the other hand, we may expect adiabatic dissociation, dissociation to atoms, when the adiabatic

TABLE IV. Approximate vibrational energy level spacing ( $\text{cm}^{-1}$ ) of the diabatic ionic states, at the energy of the corresponding atomic dissociation limit.

	F	Cl	Br	I
Li	120	100	120	140
Na	70	52	57	69
K	24	15	14	27
Rb	16	8.8	12	17
Cs	7.3	2.4	5.6	9.6

exit channel is large in comparison to the vibrational spacings, so that most molecules, with typical step sizes, enter the adiabatic channel as they climb the vibrational ladder. Four salts clearly fall into this class: LiBr, LiI, NaBr, and NaI. When we use the values of  $E_{AD}^0$  based on the analytic Hartree-Fock functions in Table II.B, LiBr and NaBr approach being intermediate cases. Several salts fall in an intermediate classification; we expect their primary dissociation products to be mixtures of both atoms and ions. For

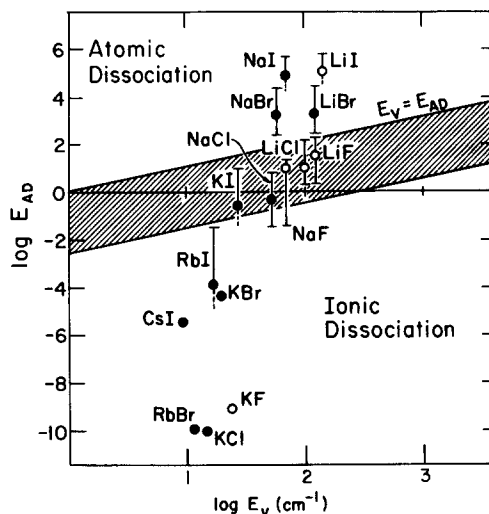


FIG. 10. Classification of the alkali halides based on the data of Tables III and IV; the plot gives  $\log(E_{AD})$  on the ordinate and  $\log(E_V)$  on the abscissa. With the possible exception of RbI, which appears from its experimental values of  $B(l)$  to be intermediate, the observed results correspond to the assignments indicated by the figure. Salts well above the line of unit slope dissociate to atoms; salts well below the line of unit slope dissociate to ions. Salts lying slightly below the line of unit slope are intermediate cases. Solid circles are used for salts for which experiments have been done; open circles indicate salts not yet studied. Only the intermediate values (c) are shown for salts well off the line of unit slope; upper and lower limits are based on (a) and (b) of Table III—for salts near the line  $E_{AD} = E_V$ . The shaded band covers the region of species giving mixed atomic and ionic dissociation. Salts not shown (CsBr, CsCl, CsF, RbCl, RbF) fall below the scale, i.e.,  $E_{AD} < 10^{-10}$ ; all of these except RbF have been studied.

these salts,  $0.1 E_{AD} < E_V < E_{AD}$ : LiCl, NaCl, NaF, LiF, KI, and possibly RbI. Any more detailed specification of the branching ratio for these salts would require wavefunctions of high accuracy, from which the off-diagonal elements  $H_{ia}$  could be calculated. The calculated branching ratios are shown in Fig. 10.

Our experimental results fit the qualitative aspects of the analysis. Those salts which we have studied that show halide ions being produced before alkali metal atoms are all salts for which  $E_V \gg E_{AD}^0$ . CsBr, CsI, CsCl, RbBr, RbCl, and KBr have been observed to produce ions before atoms, often producing maxima in

the halogen ion concentrations about 10  $\mu$ sec after passage of the reflected shock wave. Independent studies of CsF show the same behavior. By contrast, shock wave dissociation of LiBr, NaBr, and NaI produces atoms and not ions in the primary dissociation step. Indeed, the dissociation of these salts often produce a transient overabundance of ground state atoms. These salts are characterized by  $E_{AD}^0 > E_V$ . We have observed intermediate behavior in the shock dissociation of NaCl, KI, and possibly RbI. These are molecules characterized by  $E_{AD}^0 \approx E_V$ . Our model was first developed to explain the clearly intermediate behavior of KI. The model indicates that NaCl should show the intermediate, mixed dissociation. This result was, in fact, obtained from theory before it was observed experimentally.

Our experimental results for RbI are not as well documented as those for KI, largely because the very intense ( $5p \leftarrow 4s$ ) rubidium absorption line used to monitor Rb was quickly saturated in reflected shocks. Moreover, substantial absorption due to Rb was present in the incident shocks. The theory presented here predicts that the branching ratio for RbI could be three orders of magnitude smaller than that for KI. We cannot put RbI in the same class as CsI or CsBr (inverted populations of ions). On the other hand, the proportion of atoms initially produced in dissociation of RbI sometimes appeared to be greater than in KI shocks. This discrepancy between theory and experiment was not evident in a preliminary report of this work.<sup>13</sup> There we correlated the dissociation mode with the relative size of vibrational spacings and the adiabatic term splitting ( $\Delta E^0 \sim 2H_{ia}$ ),  $\Delta E^0 \cong 16 \text{ cm}^{-1}$ , rather than with the adiabatic channel width,  $E_{AD} \cong 3 \times 10^{-2} \text{ cm}^{-1}$ . On the basis of  $\Delta E^0$ , we previously expected that the branching ratio for RbI should be about a factor of 3 larger than that for KI. A comparison of the two salts based on adiabatic channel widths,  $E_{AD}$ , shows that RbI is expected to be more "ionic" than initially thought. A reinvestigation of RbI and KI using weaker absorption lines to reduce the complications of saturation and dissociation in the incident shock could provide an accurate quantitative measurement of the branching ratio. From the experiment and the theory outlined here, approximate values of  $H_{ia}$  could readily be obtained. Such a study is now in progress.

A comment on independent studies of alkali halide dissociation is in order. Wagner *et al.*<sup>4</sup> have studied the dissociation of CsCl, KCl, and NaCl by monitoring the decay of continuous molecular absorption and the rise of alkali metal excited states, as measured by alkali emission lines. The rate obtained from a series of shocks were then fit to an Arrhenius rate law. The dissociation mode, adiabatic to atoms, or diabatic to ions, was then inferred from the computed activation energies.

Their experiments point out the ambiguity of inferences drawn from activation energy data. The results implied that CsCl dissociates to ions, as our direct measurements also showed. Activation energies obtained for KCl and NaCl were interpreted to mean that these salts dissociate to atoms. Our data shows that under some conditions the initial decay of NaCl is mixed; both ions and atoms are initially formed from this salt. NaCl, like KI, is actually intermediate in its dissociation. KCl, however, is not expected to dissociate to atoms, according to our model. KCl, like KBr which we have studied, has an extremely large crossing distance, a small adiabatic term splitting and an even smaller adiabatic channel width. We believe that the inferences about curve crossing or avoided crossing in KCl drawn from activation energy measurements are misleading. The source of this error could be caused by apparent reduction of the activation energy due to the competition of vibrational ladder climbing and dissociation,<sup>6</sup> or it could be caused by poor time resolution in measuring the decay of the salt. Insufficient time resolution could effect the rate constant measurement if the dissociation mechanism at early times is replaced by another mechanism at later times, e.g., greater than about 10  $\mu$ sec. after the reflected shock has passed. According to our preliminary kinetic models, the rate of these later processes depend on the electron concentration and have no relationship at all to the initial mode of decay or the crossing or non-crossing of potential curves.

We shall not dwell here on the kinetics by which the dissociated salts relax to their thermally equilibrated population distributions. It is sufficient now to say that at least one model is consistent with our observations of alkali atom and halide ion concentrations. The models we have thus far found completely or partially successful suggest that, although the processes at early times must proceed by collisions of heavy particles, the kinetics may well be dominated by electron impact processes as soon as free electrons are present in any quantity. This is a consequence merely of the high velocities of electrons; the cross sections, e.g., for collisional detachment of electrons from negative ions by electron impact, are entirely consistent with previous results.<sup>14</sup>

\* Supported by the U.S. Army Research Office-Durham, under Grant DA-ARO-D-31-124-G1100.

† One of us (R.S.B.) wishes to acknowledge the helpful assistance of the Aspen Center for Physics, where some of this work was done.

‡ Present address: Department of Chemistry, University of Illinois, Champaign, Ill.

<sup>1</sup> J. Franck, H. Kuhn, and G. Rollefson, *Z. Physik* **43**, 155 (1927).

<sup>2</sup> R. S. Berry, *J. Chem. Phys.* **27**, 1288 (1957).

<sup>3</sup> R. S. Berry, T. Cernoch, M. Coplan, and J. J. Ewing, *J. Chem. Phys.* **44**, 127 (1968).

<sup>4</sup> V. R. Hartig, H. A. Olschewski, J. Troe, and H. G. Wagner, *Ber. Bunsenges. Physik. Chem.* **72**, 1016 (1968).

<sup>5</sup> A. Mandl, E. W. Evans, and B. Kivel, *Chem. Phys. Letters* **5**, 307 (1970).



- <sup>6</sup> J. Keck and G. Carrier, *J. Chem. Phys.* **43**, 2284 (1965).  
<sup>7</sup> H. S. W. Massey and E. H. S. Burhop, *Electronic and Ionic Impact Phenomena* (Clarendon, Oxford, England, 1952), pp. 87-88.  
<sup>8</sup> L. D. Landau, *Physik. Z. Sowjetunion* **2**, 46 (1932).  
<sup>9</sup> D. Herschbach and R. Grice (private communication).  
<sup>10</sup> D. R. Bates and A. Damgaard, *Phil. Trans. Roy. Soc. (London)* **A242**, 101 (1949).

- <sup>11</sup> D. Liberman, J. T. Waber, and D. T. Cromer, *Phys. Rev.* **137**, A27 (1965).  
<sup>12</sup> (a) P. S. Bagus, *Phys. Rev.* **139**, A619 (1965); (b) E. Clementi, *J. Chem. Phys.* **41**, 303 (1964).  
<sup>13</sup> J. J. Ewing, R. Milstein, and R. S. Berry, *Seventh International Shock Tube Symposium*, Toronto, 1969.  
<sup>14</sup> D. F. Dance, M. F. A. Harrison, and R. D. Rundel, *Proc. Roy. Soc. (London)* **299**, 525 (1967).

THE JOURNAL OF CHEMICAL PHYSICS VOLUME 54, NUMBER 4 15 FEBRUARY 1971

## Rydberg Terms of the CH<sub>3</sub> Radical\*

JONATHAN BARNARD AND A. B. F. DUNCAN†

*Department of Chemistry, University of Rochester, Rochester, New York 14627*

(Received 28 September 1970)

Spectroscopic terms are calculated for two of the three observed Rydberg series in CH<sub>3</sub>. One-center SCF functions of CH<sub>3</sub><sup>+</sup>, determined by Joshi are used for the core orbitals. The molecular geometry of CH<sub>3</sub><sup>+</sup> is assumed to be unchanged for the Rydberg states. The calculated terms are in good agreement with experimentally observed terms but suggest a possible reinterpretation of the latter.

The methyl radical, CH<sub>3</sub>, has been important as an intermediate species in chemical kinetics for a long time, but its absorption spectrum was discovered only recently.<sup>1</sup> Herzberg<sup>2</sup> discovered three Rydberg series ( $\beta$ ,  $\delta$ ,  $\gamma$ ) and interpreted the corresponding upper states in  $D_{3h}$  symmetry as  $\beta(A_1')$ ,  $\delta(A_1')$ ,  $\gamma(E'')$ . Herzberg suggested that the electron was excited to ( $nsa_1'$ ) in the  $\beta$  series and to ( $nda_1'$ ) in the  $\delta$  series. We have made calculations based on orbital excitations ( $nsa_1'$ ) and ( $nda_1'$ ) and come to a different conclusion on the orbital nature of the Rydberg states. This difference will be discussed in another section.

The ground state of CH<sub>3</sub> is described by a molecular orbital configuration as

$$(1a_1')^2(2a_1')^2(1e')^4(1a_2''), {}^2A_2''$$

and the lowest state of the ion is described by

$$(1a_1')^2(2a_1')^2(1e')^4, {}^1A_1'$$

The allowed transitions are to  $A_1'$  and  $E''$  states, but our calculations are concerned only with the  $A_1'$  transitions. All available evidence shows that the ground states and excited states which have been analyzed<sup>2</sup> are planar. Theoretical calculations<sup>3-5</sup> show that the normal state of CH<sub>3</sub><sup>+</sup> is planar. The present calculations have assumed planarity of all Rydberg states.

### PROCEDURE AND RESULTS

The symmetrical structure of CH<sub>3</sub> and the concentration of nuclear charge at the carbon center

suggest that a one-center treatment of Rydberg states is appropriate. We have adopted the one-center core of Joshi<sup>9</sup> obtained by an SCF calculation of CH<sub>3</sub><sup>+</sup>, but have used his limited set of basis functions. The total energy was lowered by only 0.15% by his extended set. We also tried a more simple core consisting of an orthonormal set of united atom orbitals, with screening parameters found by a variational method. In all cases, the position of the terms was slightly higher than those found with the Joshi core and the results will not be reported.

The method of calculation has been described in detail before<sup>6,7</sup> and will be repeated only briefly. First, a set of basis orbitals

$$\phi_{nlm} = \sum_k^n a_{kn}(klm) \quad (1)$$

are assumed as trial functions. Requirements that the  $\phi_{nlm}$  are orthonormal and orthogonal to the core orbitals are sufficient to uniquely determine the  $a_{kn}$  for any assumed set of parameters  $\zeta_{kn}$  in the normalized ( $klm$ ). The Rydberg functions  $\psi_n^R$  are defined as

$$\psi_n^R = \sum_p b_{pn} \phi_{plm}. \quad (2)$$

The summation is extended to the number of Rydberg terms desired in the calculation, 9 or 10 in most cases. The  $b_{pn}$  are found by a standard linear variation method in which the eigenvalue equation

$$H_{\text{eff}} \psi_n^R = \epsilon_n \psi_n^R \quad (3)$$

is solved. The eigenvalues  $\epsilon_n$  are the binding energies of the Rydberg electron or negatives of the Rydberg